Ethanol-Induced Condensation of Calf Thymus DNA Studied by Laser Light Scattering

K. B. Roy,[†,‡] T. Antony,[§,||] A. Saxena,[§] and H. B. Bohidar*[,§]

School of Physical Sciences and Centre for Biotechnology, Jawaharlal Nehru University, New Delhi-110 067, India

Received: August 6, 1998; In Final Form: April 2, 1999

Effect of ethanol on calf thymus DNA (CT-DNA) has been studied in the probe length scale range $3.2 \leq qR_g \leq 6.3$ in sodium chloride/sodium citrate buffer (10 mM) adjusted to pH = 7.0 with the CT-DNA concentration fixed at 2×10^{-8} M at room temperature (20 °C). The measured hydrodynamic radius R_h and radius of gyration R_g clearly indicate condensation behavior, and the plausible conformation has been inferred from the R_h/R_g ratio. A sharp conformational transition was observed at an ethanol/water concentration 40:60. The polydispersity index deduced from the width of particle size distribution shows a minima corresponding exactly to this concentration. The results are supported by UV absorption studies done at $\lambda = 260$ nm.

I. Introduction

Condensation of DNA is known to arise from two processes, charge neutralization of the DNA phosphate charge and reduction in the water activity through the reduction in the dielectric constant of the medium. Manning's condensation theory explains cation-induced condensation of DNA molecules mostly by neutralizing the DNA phosphate charge.[1,2] The onset of condensation occurs when ~80% of the charge neutralization is complete. Laemmli[3] has shown that polyethylene oxide and polylysine induce condensation and substantial chain folding in high molecular weight DNA. Lerman[4] studied the condensation of T4 and T7 DNA induced by the presence of nonpolar polymers, polyvinyl pyrrolidinone and polyethylene oxide. Sedimentation studies showed that at low DNA concentrations phage DNA molecules collapsed into particles almost approaching the compactness of the contents of phage heads. It is generally held that several factors influence the DNA condensation and aggregation.[5,6] In addition to the electrostatic forces, these include bending or kinking, polymer chain entropy, hydration forces,[7,8] and even cross-linking by condensing ligands.[9]

Arscott et al.[1] investigated in detail condensation of DNA by multivalent cations (Co^{3+}) in alcohol/water mixtures of varying dielectric constants (ϵ) by total light scattering, CD spectroscopy, and electron microscopy. They found the scattered intensity to peak at $\epsilon = 70$ (21.7% ethanol) and thereafter decrease, but no explanation was offered. The critical concentration of Co^{3+} required to induce DNA condensation decreased from 21 to 16 μM as ϵ decreased from 80 to 70. The morphology of DNA condensate as seen in an electron micrograph changed from 93% toroids at $\epsilon = 80$ to 89% rods at $\epsilon = 70$ to 98% rods at $\epsilon = 65$, beyond which DNA condensed into a network of multistranded fibers. In their system, the B → A conformational transition of DNA took place in an ethanol concentration range of 30−40% (v/v) ($\epsilon = 70-60$) much below the usual 70% ethanol concentration ($\epsilon = 40$) observed for such transition; this was interpreted as that Co^{3+} ions and ethanol synergistically induced a B → A transition at a much lower ethanol concentration. Sedimentation behavior of DNA in an ethanol/water mixture in the absence of any condensing agent like Co^{3+} had been studied earlier by Potaman et al.,[10] who concluded that the B → A transition takes place, in such conditions, in the range of 65−80% ethanol (v/v) and such transition or corresponding CD spectral changes are independent of the aggregation process.

Very recently, using a new mechanicochemical method Piskur and Rupprecht[11] have studied thermal stability and structure of aggregated DNA in ethanol/water solution with the following significant observations. At a critical ethanol concentration, depending on the nature and concentration of counterions, aggregation of DNA sets in with marked increase in T_m over 50−60% ethanol (v/v) with DNA being still in the B-form structure. The T_m of aggregated DNA, in general, decreases with further increase in ethanol concentration but is dependent on the nature but not on the concentration of the counterion. When the ethanol concentration reaches the range of 70−80% (v/v), the B → A transition occurs in the case of Na−, K−, and CS−DNA, and the midpoint of transition is at 76% ethanol for Na−DNA, beyond which the A-form strongly promotes interhelical contacts and consequent condensation and decrease in T_m.

In the present work, we report static and dynamic light scattering (SLS and DLS) measurements on calf thymus DNA in the ethanol/water mixtures in the absence of any multivalent cations to observe and quantify CT-DNA condensation at room temperature (20 °C). We observed a sharp structural transition of DNA occurring at 40% ethanol concentration.

II. Experimental Procedures

a. Materials and Methods. Calf thymus DNA was bought from Sigma Chemicals (Cat. no. D1501, Type-1, sodium salt of highly polymerized calf thymus DNA containing less than 3% protein) with nominal molecular weight 8.6×10^6 Da. The lyophilised high molecular weight DNA was dissolved in a buffer (sodium chloride/sodium citrate buffer (10 mM), and the pH was adjusted to 7.0) containing EDTA dialyzed against the same buffer with/without EDTA. DNA was not purified any further. Dilution was done with the same buffer. The stock solution was prepared with a concentration 2×10^{-8} M, and

* Corresponding author. E-mail: bohidar@jnuniv.ernet.in.
[†] Centre for Biotechnology.
[§] School of Physical Sciences.
[||] Present Address: Department of Biophysics, University of New Jersey.

10.1021/jp983306p CCC: $18.00
Published on Web 05/27/1999

TABLE 1: Measured Total Intensity I_T Measured at $\theta = 90°$, Polydispersity, P, Diffusion Coefficient, D_T, Hydrodynamic Radius, R_h, and Radius of Gyration, R_g, for DNA in Various Concentrations of Ethanol in an Ethanol + Water Solution

ethanol (%)	I_T (au)	P	$D_T \times 10^8$ ($cm^2\ s^{-1}$)	R_h (nm)	R_g (nm)	R_h/R_g
0	0.52 ± 0.02	0.16 ± 0.02	1.86 ± 0.07	120 ± 10	180 ± 15	0.66
20	0.44 ± 0.02	0.20 ± 0.02	2.06 ± 0.08	110 ± 10	160 ± 15	0.69
40	0.39 ± 0.01	0.10 ± 0.02	2.35 ± 0.07	95 ± 8	105 ± 10	0.90
60	0.32 ± 0.01	0.21 ± 0.02	3.00 ± 0.08	75 ± 6	98 ± 8	0.77
80	0.27 ± 0.01	0.20 ± 0.02	3.45 ± 0.09	65 ± 5	90 ± 7	0.7

the aliquots were filtered through a 0.45 μm Millipore filter to remove dust. The size of DNA was measured before and after filtration to check possible degradation of DNA molecules. The sizes measured by light scattering were identical, and the samples were directly loaded into 5 mL cylindrical quartz tubes sealed with Teflon screw caps. Ethanol was spectroscopic grade reagent bought from Merck (Germany), and the desired amount of ethanol was directly loaded into the sample tube using a microsyringe. The glassware used in this experiment was precleaned with liquid detergent and dried in the oven overnight, and the sample preparation and loading were done in a dust-free chamber.

The light scattering setup consisted of a laboratory goniometer with two arms. The excitation source was a He−Ne laser (AEROTECH, 10 mW) mounted on the fixed arm of this goniometer and a photomultiplier tube was mounted on the other arm. The (dynamic light scattering) DLS experiments were carried out in the scattering angle range 20°−140° at 5° intervals. The sample was contained in a quartz cylindrical cell placed inside a homemade temperature controller.[12] The scattered light from the sample was detected by a photomultiplier tube, and the photocurrent was suitably amplified and digitized by an amplifier/discriminator before it was fed to a digital photon correlator (Brookhaven BI-9000 AT model). The whole scattering setup was installed on a vibration isolation table. The difference between the measured and calculated baseline was not permitted to exceed 0.1% for any correlogram. Data that did not conform to this was rejected.

The temperature of the sample was fixed at 20 °C and monitored with an accuracy of ±0.1 °C. Each correlogram was recorded over the time duration of typically 30 min, and over this experimental duration the temperature was observed to remain steady within the accuracy of experimental error. The pH and concentration of each of the samples was measured before and after the end of the light scattering experiments, and within the experimental error, they were found to have remained the same. The values of refractive index n and viscosity η_o of the solvent at different alcohol concentrations were taken from ref 13 and used in the calculations of particle size.

For (static light scattering) SLS measurements, scattered light was collected at 5° intervals in the scattering angle range 20°−40°. The SLS data was analyzed through the Guinier plot software supplied by Brookhaven Instruments, and similarly DLS data was analyzed through the CONTIN software provided by the same company. The parameter "probability to reject, P" was set closest to 0.5 for all samples. The UV studies were done using a Perkin-Elmer Lambda 2 UV/visible spectrophotometer in the scanning mode. After the spectral profile was obtained, the absoption data were taken at $\lambda = 260$ and 320 nm.

b. Static Light Scattering Data Analysis. The signal background was determined with benzene as the reference liquid. The total intensity of the light scattered was measured as a function of the scattered wavevector $q = 4\pi n\lambda^{-1} \sin(\theta/2)$ (by changing the scattering angle θ), where n is the refractive index of the sample and $\lambda = 6328$ Å. The background subtracted scattered intensity $I_s(q)$ can be represented as

$$I_s(q) = ACMP(q)/(\partial\mu/\partial C)_{T,P} \tag{1}$$

where μ is the excess chemical potential of the solvent due to the presence of solute in concentration C, and this can be expressed as a virial series in $C\mu = A_1C + A_2C^2 + ...$ For dilute solutions, $(\partial\mu/\partial C)_{T,P}$ is independent of C. A is an instrumental constant, and M is the molecular weight of the DNA molecules. $P(q)$ is the static structure factor and for random coils assumes the form

$$P(q) \cong \left(1 - \frac{q^2 R_g^{\,2}}{3} + ...\right) \tag{2}$$

For our experimental situation $qR_g < 1$ was valid only for scattering angles $\theta \leq 35°$. Correspondingly, $I_s^{-1}(q)$ was plotted as a function of q for θ values $\leq 35°$ and fitted to

$$\frac{1}{I_s(q)} \cong \frac{1}{ACM}\left(1 + \frac{q^2 R_g^{\,2}}{3}\right) \tag{3}$$

which yielded the value of radius of gyration R_g (Guinier plot). These values are listed in Table 1. At higher values of q, the curvature of the $P(q)^{-1}$ plot gives information about the higher moments of the polymer segment distribution, which under suitable conditions can yield indications of the actual molecular shape.

c. Dynamic Light Scattering Data Analysis. For scatterers following Brownian dynamics, the temporal electric field auto correlation function of the scattered light is given as[14−16]

$$g_1(\tau) = g_1(0) \exp(-D_T q^2 \tau) \tag{4}$$

where the translational diffusion coefficient D_T of the macromolecules is probed on a length scale q^{-1}. $g_1(0)$ is the coherence area factor, and normally in experimental situations $g_1(0) < 1$. It defines the signal-to-noise ratio and hence the quality of the correlogram. For dilute solutions and $qR_g \leq 1$, the above expression always retains the given form. For $qR_g > 1$, several relaxation modes contribute to the autocorrelation function $g_1(\tau)$ simultaneously. For those situations, $g_1(\tau)$ can be expressed as a multiexponential function.[14,15] For larger particles, separation of the internal mode from the correlation function data becomes extremely difficult. Hence, we refrain from doing so. The particle size distribution $G(\Gamma)$ can be obtained by taking a Lapalce inversion of $g_1(\tau)$,

$$G(\Gamma) = \int g_1(\tau) \exp(-\Gamma\tau)\, d\Gamma \tag{5}$$

where $\Gamma_i = D_i\, q^2$ for the ith diffusing particle, and the above integral runs over all particle sizes. The experimentally measured intensity correlation function $g_2(\tau)$ was reduced to $g_1(\tau)$ using the Siegert relation[14] $g_2(\tau) = a + b|g_1(\tau)|^2$ where 'a' was the

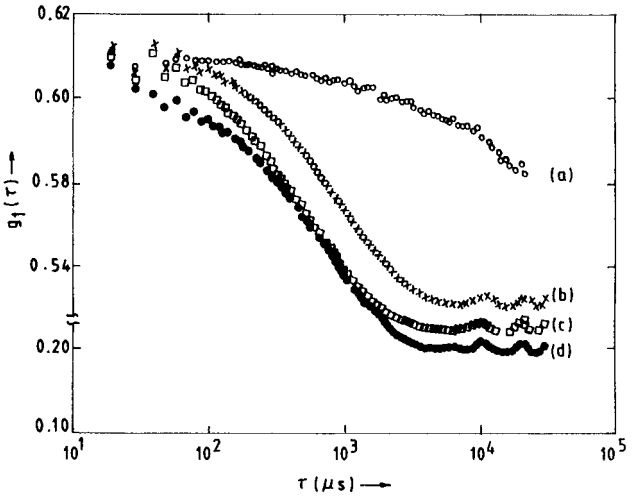

Figure 1. The field autocorrelation function $g_1(\tau)$ as a function of ethanol concentration for CT−DNA molecules in sodium chloride/sodium citrate, pH = 7.0 solution at $T = 20$ °C. Curves a, b, c, and d correspond to 0%, 40%, 60%, and 80% concentrations of ethanol. Notice the abrupt change in the width of $g_1(\tau)$ at 40% ethanol concentration implying formation of condensates.

background of the signal at $\tau \rightarrow \infty$ and '*b*' was the coherence area factor. The ratio *b*/*a* defines the signal modulation. A good correlogram demands a signal modulation of at least 50%. The correlation data were subjected to CONTIN analysis (probability to reject = 0.5), and the particle size distributions were obtained. This gave the mean particle size of the condensates. The deduced values of D_T are given in Table 1. The hydrodynamic radius R_h was deduced using the Stokes equation

$$D_T = \frac{k_B T}{6\pi\eta_o R_h} \tag{6}$$

where k_B is the Boltzmann constant and η_o is the solvent viscosity at absolute temperature *T*.

III. Results and Discussions

The total scattered intensity shows a distinct peak at ~40% alcohol concentration with features qualitatively identical to that of Arscott et al.[1] The total light scattered from the DNA molecules I_T can be written as the sum of the light scattered from the translational motion I_d of the macromolecule and the internal mode relaxations I_i, ($I_T = I_d + I_i$). However, these values could not be computed in our experiments. Some representative I_T values obtained at $\theta = 90°$ are listed in Table 1.

Typical correlation functions are shown in Figure 1. As the alcohol concentrations was increased, the figure shows significant shrinking of the correlogram width, qualitativly implying scattering from smaller particles and onset of condensation. The translational and internal relaxation modes can in principle be separated by assuming a double exponential relaxation for $g_2(\tau)$ and by plotting the relaxation times as a function of q^2. However, this extrapolation method fails to give reliable information for larger polymers such as DNA. Figure 2 shows the variation of hydrodynamic radius and translational diffusion coefficient D_T as a function of ethanol concentration. The variation of absorption at $\lambda = 260$ nm and 320 nm is shown in Figure 3. The decrease in absorption at $\lambda = 260$ nm and the corresponding increase in scattering at $\lambda = 320$ nm at alcohol concentration ~40% imply the formation of connensates in the system. The most significant result in this study is that the value of the

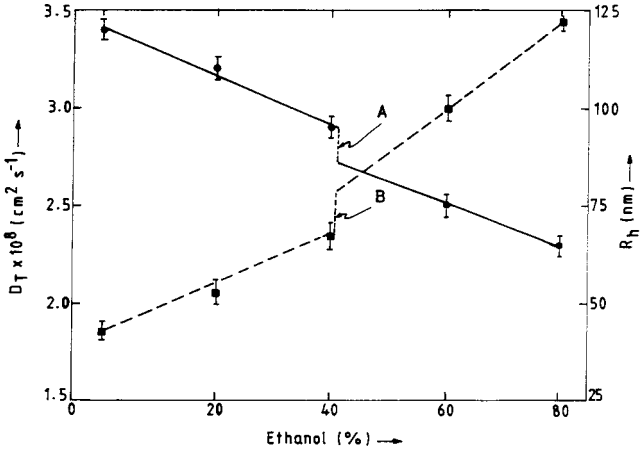

Figure 2. Variation of translational diffusion coefficient D_T and hydrodynamic radius R_h of CT-DNA molecules as a function of increasing ethanol concentration in sodium chloride/sodium citrate, pH = 7.0 solution at $T = 20$ °C. Note the sudden drop (A) in the R_h value close to an ethanol concentration of 40% and the sudden jump (B) in the D_T value at the same point. See Table 1 for details.

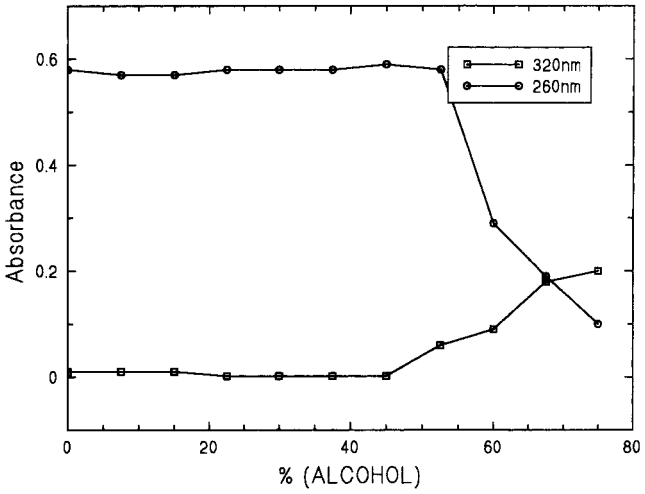

Figure 3. Variation in the UV absorption of CT−DNA as a function of increasing ethanol concentration in sodium chloride/sodium citrate, pH = 7.0 solution at $T = 20$ °C. Note the sudden drop in absorption value at $\lambda = 260$ nm close to an ethanol concentration of 40% (due to formation of condensates) and the sudden jump in same at $\lambda = 320$ nm at the same point implying enhanced scattering.

translational diffusion coefficient D_T shows a sharp jump close to an ethanol/water ratio of 40:60, thereby indicating a conformational transition, presumably structural, but it is not a B → A transition as judged by the CD spectra (not shown).

Correspondingly, the hydrodynamic radius, R_h, exhibits a sharp jump at the same ethanol concentration. The values of both R_h and R_g fell by almost 50% at the highest ethanol concentration (see Table 1). As the alcohol percentage was increased the dielectric constant of the solvent medium decreased gradually, thus making the environment conducive to the initiation of DNA condensation. Similar observations have been made earlier too.[17−19] The R_h/R_g values listed in Table 1 are indicative of the three-dimensional conformation of the macromolecule. For a Gaussian chain[20] $R_h/R_g = 0.665$, which was observed for DNA in the absence of any alcohol. As the ethanol concentration was raised, this ratio increased to 0.90 at 40% alcohol and then fell to 0.70 at 80% ethanol concentration. For a spherical condensate R_h/R_g will be ≅1.3. The data in Table 1 imply that the condensates do tend to get more compact,

possibly ellipsoids if not spherical, as the ethanol concentration reaches 40%, and the compactness gets lost at higher concentrations of alcohol. These sharp changes in structure and shape of DNA molecules at 40% alcohol concentration are just before the critical concentration when aggregation sets in (Figure 3) and resemble what Arscott et al.[1] observed at $\epsilon = 70$, which corresponds to 21.7% ethanol concentration. The width of the particle size distribution curve gives the polydispersity index P of the solute particles. As has been shown in Table 1, P showed a minima at 40% alcohol concentration, implying a narrowed distribution of diffusing particles, which we identify as condensates. The value of P was found to be much larger at ethanol concentrations both lower and higher than 40%.

They observed[1] total scattering intensity peaked at $\epsilon = 70$, and electron micrographs showed distinct rod shaped molecules, which were absent at $\epsilon = 65$ or 75. These were interpreted as fold-backs of B-form DNA, which strongly adheres, rapidly aggregating into a fibrous network when ϵ reaches a value of less than 60. We believe that the sharp changes we observe at 40% ethanol concentration ($\epsilon \sim 60$) represent some sort of structural transition from normal B-DNA to a more compact form within the same B-family of structures. For example, the axial rise of normal B-DNA is 3.4 Å, whereas D-DNA within the B-family has an axial rise of 3.03 Å. The more compact A-DNA has an axial rise of 2.56 Å, and these strongly self-adhere. Possibly compactness promotes aggregation. Normal B-DNA is thought to be stabilized by two layers of water molecules forming a so-called spine of hydration in narrow minor groove. It has been argued that a B → A transition occurs when this spine of hydration is removed at low water activity. It is plausible that at a critical ethanol concentration (and critical water activity) the outer hydration shell breaks down thereby destabilizing and changing B-DNA to a more compact form so that interhelical interaction increases and aggregation sets in. Such a scenario brings our results and those of Piskur et al.[11] in total agreement and can also explain scattering maxima at $\epsilon = 70$ observed by Arscott et al.[1] albeit at 21.7% ethanol concentration. Conformational transitions in DNA are known to be induced by alcohol as well as by $Co^{3+}(NH_3)_6$, and the two agents may act synergistically. The B → A transition was induced by alcohols at 70% ethanol for Na−DNA[11] but at 30−40% ethanol in the presence[1] of $Co^{3+}(NH_3)_6$, showing the same synergesis.[1] Therefore, what we observe at 40% ethanol concentration in the absence of any other condensing agent might be happening at 21.7% ethanol in the presence of Co^{3+}. Thus, our results are in agreement with those reported by Piskur et al.[11] and Arscott et al.[1] Qualitative features of our work and that of Arscott et al. also agree. Like them, we also observe three distinct regimes of condensation. Below 40%, the flexible chains possibly condense as toroids, at 40%, a compact ellipsoidal structure forms followed by aggregation, and at still higher alcohol concentration, we do observe the third regime when the R_h/R_g ratio decreases sharply, possibly due to formation of an open network structure of self-adhering A-DNA (Figure 4).

The dielectric constant of the ethanol/water mixture decreases[13] from ~75 at 10% ethanol concentration to ~50 at 60% concentration, and at still higher ethanol concentration the dielectric constant falls well below 40. It has long been realized that a critical fraction of DNA charge must be neutralized effectively before condensation can be initiated.[21] Wilson and Bloomfield[22] have quantitatively studied the effect of multivalent ions in neutralizing DNA phosphate charge using Manning's counterion condensation theory.[2] This theory infers that at 25 °C monovalent ions can neutralize 76% of phosphate charge. Another interesting observation of the theory is that DNA condensation can occur when cations neutralize ~80% of the DNA phosphate charge in aqueous solutions and in a 50% (v/v) water/methanol solution.

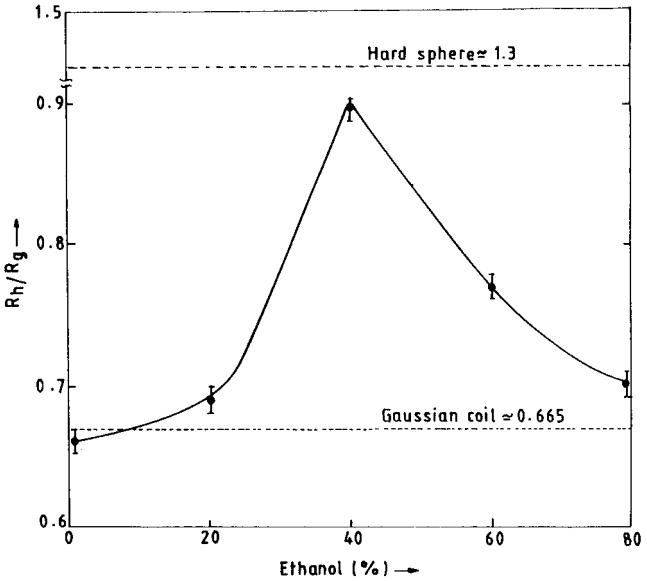

Figure 4. Variation of R_h/R_G for CT−DNA molecules as a function of ethanol concentration. For a hard sphere $R_g^2 = (2/5)R_h2$ and for a Gaussian coil $R_h = 0.665R_g$. These are shown as dotted lines. See Table 1 for details.

An estimate of Coulombic driving forces facilitating DNA condensation can be derived from the Oosawa theory[23] of fluctuating counterion atmosphere surrounding the DNA molecule. Another contention has been that hydrodynamic forces dominate electrostatic behavior when DNA helices approach closer than a few water diameters.[24] Apart from altering the dielectric constant of the dispersion medium, the effect of ethanol is presumably due to its dehydrating action, since lower water activity is known to favor the formation of DNA condensates. Nonetheless, the compact DNA configurations observed in vivo are largely stabilized through positively charged proteins. These protein molecules effectively neutralize the negative charges on DNA phosphates, thus reducing the Coulombic forces that hinder close packing (condensation).

IV. Conclusion

The objective of this work was to see the effect of ethanol on DNA phosphate charge neutralization and the eventual condensation of DNA molecules. The experiments were perfomed in the probe length scale region $3.2 \leq qR_g \leq 6.3$, where Pecora's calculations[25] show that higher modes contribute significantlly to the internal relaxation of the DNA molecule. The DLS spectra could be well discussed through a double exponential function.[26] The R_h/R_g ratio provided an indicator to the plausible three-dimensional conformation of the macromolecule, and we observed this ratio conforming to that of a Gaussian coil at low alcohol concentration, an abrupt shape transition at 40% ethanol concentration where the ratio conformed to a value closer to that of an equivalent sphere. At higher alcohol concentration, the Gaussian chain behavior manifested again. Light scattering data does not provide any indication about the possible three-dimensional conformation of DNA at an ethanol concentration of 80%. Second, our data could not decipher between a hard sphere and a toroid.

References and Notes

(1) (a) Arscott, P. G.; Ma, C.; Wenner, J. R.; Bloomfield, V. A. *Biopolymer* **1995**, *36*, 345; (b) **1990**, *30*, 619.
(2) Marquet, R.; Houssier, C. *J. Biomol. Struct. Dyn.* **1991**, *9*, 159.
(3) Bloomfield, V. A. *Biopolymers* **1991**, *31*, 1471.
(4) Rau, D. C.; Parsegian, V. A. *Proc. Natl. Acad. Sci. U.S.A.* **1984**, *81*, 2621.
(5) Rau, D. C.; Parsegian, V. A. *Biophys. J.* **1992**, *61*, 246.
(6) Schellman, J. A.; Parthasarathy, N. *J. Mol. Biol.* **1984**, *175*, 313.
(7) Manning, G. S. *Biopolymers* **1990**, *19*, 37. Manning, G. S. *Quart. Rev. Biophys.* **1978**, *11*, 179.
(8) Laemmli, U. K. *Proc. Natl. Acad. Sci. U.S.A.* **1975**, *72*, 4288.
(9) Lerman, L. S. *Proc. Natl. Acad. Sci. U.S.A.* **1971**, *68*, 1886.
(10) Potaman, V. A.; Banikov, Y. A.; Shlyaehtenko, L. S. *Nucleic Acid Res.* **1980**, *8*, 635.
(11) Piskur, J.; Rupprecht, A. *FEBS Lett.* **1995**, *375*, 174.
(12) Bohidar, H. B.; Berlend, T.; Jossang, T.; Feder, J. *Rev. Sci. Instrum.* **1987**, *58*, 1422.
(13) *CRC Handbook of Chemistry and Physics*, 63rd ed.; Boca Raton: FL, 1983.
(14) Bloomfield, V. A.; Crothers, D. M.; Tinoco, I., Jr. *Physical Chemistry of Nucleic Acids*; Harper and Row: New York, 1974.
(15) Berne, B. J.; Pecora, R. *Dynamic Light Scattering*; Wiley-Inter Science: New York, 1976.
(16) Chu, B. *Laser Light Scattering*; Academic Press: New York, 1974.
(17) Ma, C.; Bloomfield, V. A. *Biophys. J.* **1984**, *67*, 1678.
(18) Benbasat, J. A. *Biochemistry* **1984**, *23*, 3609.
(19) Votavova, H.; Kucerova, D.; Felsberg, J.; Sponar, J. *J. Biomol. Struct. Dyn.* **1986**, *4*, 477.
(20) Yamakawa, H. *Modern Theory of Polymer Solutions*; Harper and Row: New York, 1971.
(21) Marquet, R.; Houssier, C. *J. Biomol. Struct. Dyn.* **1991**, *9*, 159.
(22) Wilson, R. W.; Bloomfield, V. A. *Biochemistry* **1979**, *18*, 431.
(23) Oosawa, F. *Polyelectrolytes*; Marcel Dekker: New York, 1971.
(24) Leikin, S.; Parsegian, V. A.; Rau, D. C.; Rond, R. P. *Annu. Rev. Phys. Chem.* **1993**, *44*, 369.
(25) Pecora, R. *J. Chem. Phys.* **1965**, *43*, 1562; **1968**, *49*, 1032.
(26) Jolly, D.; Eisenberg, H. *Biopolymers* **1976**, *15*, 61.